International Journal of Rock Mechanics & Mining Sciences xxx (xxxx) xxx–xxx

Contents lists available at ScienceDirect

International Journal of Rock Mechanics & Mining Sciences

journal homepage: www.elsevier.com/locate/ijrmms

Evaluation and reduction of the end friction effect in true triaxial tests on hard rocks

Xia-Ting Feng[a], Xiwei Zhang[b,*], Chengxiang Yang[b], Rui Kong[b], Xiaoyu Liu[b], Shuai Peng[b]

[a] State Key Laboratory of Geomechanics and Geotechnical Engineering, Institute of Rock and Soil Mechanics, Chinese Academy of Sciences, Wuhan 430071, China

[b] Key Laboratory of Ministry of Education on Safe Mining of Deep Metal Mines, Northeastern University, Shenyang, Liaoning 110819, China

ARTICLE INFO

Keywords:
True triaxial testing
Hard rock
End friction effect
Antifriction
Effect
Stearic acid

1. Introduction

Since Von Kármán[1] first published conventional triaxial test data on rocks in 1911, the primary installation method has consisted of using a cylindrical specimen sandwiched by two metal platens. The mismatch in the elastic parameters (Young's modulus and Poisson's ratio) between the metal platens and rock specimen in the elastic and yielding ranges produces an interface friction when axially loaded, which results in a non-uniform stress distribution at the end of the specimen; this situation is defined as the end friction effect. Lubrication is an effective method to decrease the friction between opposing solid faces by applying a solid or fluid anti-friction agent. To reduce the end friction effect in rock mechanics uniaxial or conventional triaxial compression tests, anti-friction agents, such as “stearin” or stearic acid,[2] a Teflon sheet,[3] Teflon and copper sheets,[4,5] and low-modulus insert materials,[6] have been widely used. The theoretical solution method has been employed to analyse the stress distribution within a circular cylinder, in which the friction coefficient and boundary condition were considered.[7–9] Labuz and Bridell[10] proposed a new friction constraint reduction method in uniaxial compression tests and published the coefficients of friction of the anti-friction agent and deformation effect on the specimen. To date, no established or standard methods similar to ISRM[11] and ASTM[12] have been reported regarding ways to eliminate the end friction effect in rock compression tests.

Recently, the influence of the end friction effect has been presented and discussed in a number of professional rock mechanics tests such as shear tests,[13] split Hopkinson pressure bar tests[14] and true triaxial tests.[15] True triaxial tests can replicate the general stress state ($\sigma_1 > \sigma_2 > \sigma_3$)[16–20] in rock crust; thus, research needs have driven the development of true triaxial testing apparatuses. However, the end friction effect is more complex than the stress state observed in conventional triaxial apparatuses because more friction interfaces arise during specimen loading in the multi-axis configuration.

Mogi[21] directly applied a Teflon sheet, and Haimson and Chang[17] applied a mixture of stearic acid and Vaseline (MSV) with a thin copper sheet in their true triaxial tests. Furthermore, some numerical tools were also used to verify and quantify the end friction effect in true triaxial tests.[22–24] The friction mechanism and contact modelling of the end friction effect in true triaxial testing is complex, so some parameters and modelling have been simplified, which could affect the extraction of the influence mechanism from the numerical work. The stress distribution in the specimen is expected to be homogeneous in the design of a true triaxial apparatus.[21]

2. End friction effect and lubrication in true triaxial testing

Bowden noted that friction properties are influenced by material, temperature, rate of movement, area of contacts and surface films.[25] The function of the anti-friction agent is to form an intermediate film to separate the solid surfaces. Labuz and Bridell[10] determined the friction coefficients for graphite, double-sheet Teflon, a stearic acid and Vaseline mixture and alloy steel platens to be approximately 0.07–0.08, 0.05 and 0.02, respectively. Recently, an ethylene glycol material

* Corresponding author.
E-mail address: zhangxiwei@mail.neu.edu.cn (X. Zhang).

http://dx.doi.org/10.1016/j.ijrmms.2017.04.002
Received 3 March 2016; Received in revised form 30 March 2017; Accepted 15 April 2017

with attached hydrogen ions with an ultra-low friction coefficient (μ=0.004), placed been between Si_3N_4 and SiO_2, was reported,[26] but it has not yet been applied in rock mechanics compression tests.

The cylindrical specimen is axially loaded by the matched top and bottom alloy steel platens, and the ideal deformation is proportionally shortened in the axial direction and proportionally expanded in the radial direction to maintain the original cylinder shape. However, due to the end friction effect, a barrel-shaped specimen is often obtained, especially for soft rocks and soils. Furthermore, the friction stress distribution is not uniform on the end plane because the relative motion in the centre approaches zero; conversely, a relatively large motion arises at the edge of the sample, possibly linked to a transition from static friction to kinetic friction. With respect to end friction, Ferrero and Migliazza reported maximum values at the edge and minimum values at the centre of the specimen.[27]

In true triaxial tests, however, a rectangular prismatic specimen with an approximate length-width-height ratio of 1:1:2 or 1:1:1 was rigidly loaded on four surfaces[6,17,18] or six surfaces.[19] The intermediate principal stress (σ_2) acts on two rectangle surfaces, which produces an additional end friction effect. Although there is no rigid contact on the front and back surfaces when the fluid pressure produces the minor principal stress σ_3, the deformation is affected by the end friction effect resulting from the rigid loading. Consequently, the end friction effect must also be evaluated for the interface subjected to σ_2.

The end friction in true triaxial tests can be characterized at room temperature with small compression strain rates (approximately 10^{-5}/s), a high normal stress (up to hundreds of MPa), and plane friction consisting of a combination of static and dynamic friction. Because little comparative research has been conducted to investigate the end friction effect in true triaxial tests, some researchers have applied an anti-friction agent directly to the interface during testing, but the influence of the end effect on the deformation was not reported in detail. This study presents an evaluation of the end friction effect in true triaxial rock tests in view of this lack of research, with the goal of developing a proper approach for reducing end friction in true triaxial testing.

3. Experimental apparatus and method

A newly developed true triaxial apparatus combining rigid and flexible loading was used to evaluate the end friction effect experimentally [20]. A multi-point strain measurement method is proposed to evaluate the elastic strain distribution induced by the end friction effect. Strain rosette gauges are glued on the free face of the specimen to measure the deformation. Two elements are attached at one point such that the compression and expansion strain can be measured. A data logger (UCAM-60A, Kyowa Electronic Instruments, Chofu, Tokyo) was used to measure the strain signal.

All steel and granite rectangular prismatic specimens were machined to be 50×50×100 mm^3, and a grinding machine was used to polish the specimen surface. The dimensional tolerance and perpendicular tolerance are given as ± 0.01 mm and 0.02 mm, respectively, for each side. The Young's modulus (E) and Poisson's ratio (μ) for the alloy steel platen, steel specimen and granite specimen were determined in uniaxial compression to be approximately 230 GPa and 0.28, 208 GPa and 0.30, and 65 GPa and 0.25, respectively. A series of experiments were performed to investigate the end friction effect in the rue triaxial apparatus.

4. Results and discussion

4.1. Measurement of the friction coefficient

The friction coefficients of granite, Teflon, a composite of Teflon and MoS_2 (Dow Corning Molykote BR2 plus), and MSV against the alloy steel platen were measured in a true triaxial apparatus that was modified to function in a double direct-shear mode. The mixture of stearic acid and Vaseline (MSV) was prepared at a weight ratio of 1:1 by melting at 70 °C. Stearic acid is a fatty acid and thus acts as a solid lubricant, and Vaseline is added for ease of application; details were presented by Labuz and Bridell.[10] The same alloy steel platen and a shear rate of 0.005 mm/s were used in all tests.

There are two friction interfaces to balance the shear force in the tests, so the calculation of the friction coefficient is represented by

$$\mu = F/2N \tag{1}$$

where μ is the friction coefficient, F is the shear force, and N is the normal force.

The static friction coefficients that correspond to the onset of the bulk sliding of the specimen were measured under various normal loading forces of 25–200 kN. The static friction coefficients of the granite, Teflon, composite of Teflon and MoS_2, and MSV are plotted in Fig. 1. Each point in the figure represents the average value of three measurements, and the error bars indicate the standard deviation. Because of the very effective surface smoothing of the granite specimens, the friction coefficient between the granite and alloy steel platen was low and ranged from 0.146 to 0.157. The friction coefficients of the Teflon, the composite of Teflon and MoS_2, and the MSV tend to depend slightly on the normal loading force: the friction coefficient decreases with increases in the normal loading force. Linker and Dieterich reported the effects of variable normal stress on rock friction without using an anti-friction technique.[28] The mean friction coefficients for all the points of the Teflon, composite of Teflon and MoS_2, and MSV are 0.043, 0.021 and 0.018, respectively. The MSV exhibits a lower friction coefficient than the other interfaces due to its formation of a hydrodynamic film between the two sliding surfaces. The results of the composite of Teflon and MoS_2 shows a slightly raised friction coefficient under low normal forces; however, with increasing normal stress, the friction coefficient becomes smaller than that of the MSV. To obtain a uniform effect, the use of the composite of Teflon and MoS_2 is not suggested, and MSV instead is suggested for use in true triaxial compression testing.

4.2. End friction effect under loading in the short-axis direction

The end friction effect under loading in the short-axis direction is related to the direction of the intermediate principal stress loading in true triaxial tests, which features an additional end friction interface relative to the conventional triaxial tests. The MSV with a 0.02-mm-thick copper sheet was placed between the alloy steel platen and the specimen, on which the copper sheet was set. The strain at central point 2 was selected as a reference datum. Typical end constraint deformation can be observed for both the steel and granite specimens at the edges of the specimens (point 4 and 5). The compression strain

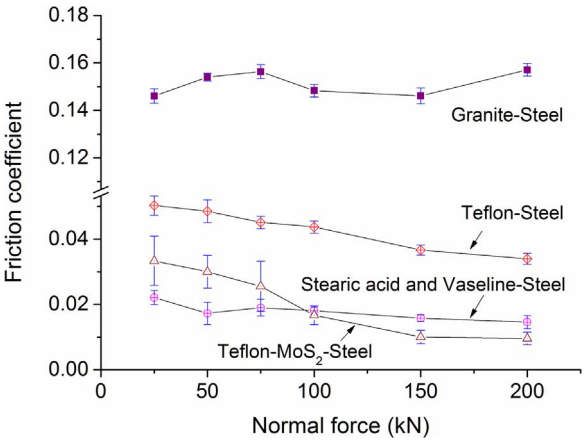

Fig. 1. Friction coefficient vs. normal loading force.

at the edge is deflected from the centre point, and this apparent end friction effect is shown in Fig. 2(a). When using the MSV, the deformation at the edge of the sample significantly converges at the centre line for the steel specimens and slightly converges for the rock specimens, as shown in Fig. 2(b). When the loading is applied in the long-axis direction and the height/width ratio is 2, the convergence of the deformation is much better than that when the loading is applied in the short-axis direction and the height/width ratio is 0.5. The differences in the deformation and elasticity parameters are related to the different loading directions, or, more precisely, they are an effect of the slenderness. As reported previously,[29–33] the elastic modulus increases with an increase in the height/width ratio.

Regardless, the end friction effect is reduced when using the MSV in the loading direction of the intermediate principle stress. The deformation and elastic parameters present slight deviations due to the height/width ratio, which is inevitable because of the loading in the short-axis direction when using the rectangular prismatic specimen.

4.3. End friction effect under the biaxial loading pattern

True triaxial tests often employ a loading path in which σ_1 and σ_2 are simultaneously and gradually increased to a desired σ_2 level; therefore, the end friction effect under this biaxial loading pattern was investigated as well. The deformation in both the long- and short-axis directions presents compression strain due to biaxial loading; the stress–strain curves for three measurement points for granite speci-

Table 1
Uniaxial compression strengths (MPa) when using various anti-friction agents.

Specimen	Without an anti-friction agent	With one layer of Teflon	With MSV
Granite	171.05 ± 6.1	153.02 ± 4.1	161.42 ± 8.9
Marble	71.98 ± 2.5	62.16 ± 1.6	66.1 ± 1.95

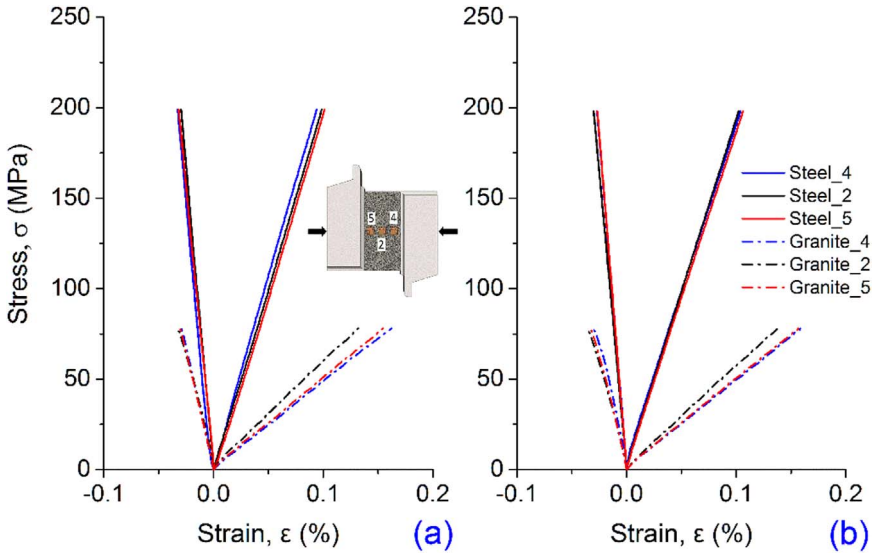

Fig. 2. Stress–strain curves of rectangular prismatic specimens for steel and granite specimens for loading in the short-axis direction: (a) with end friction; (b) stearic acid and Vaseline with a copper sheet.

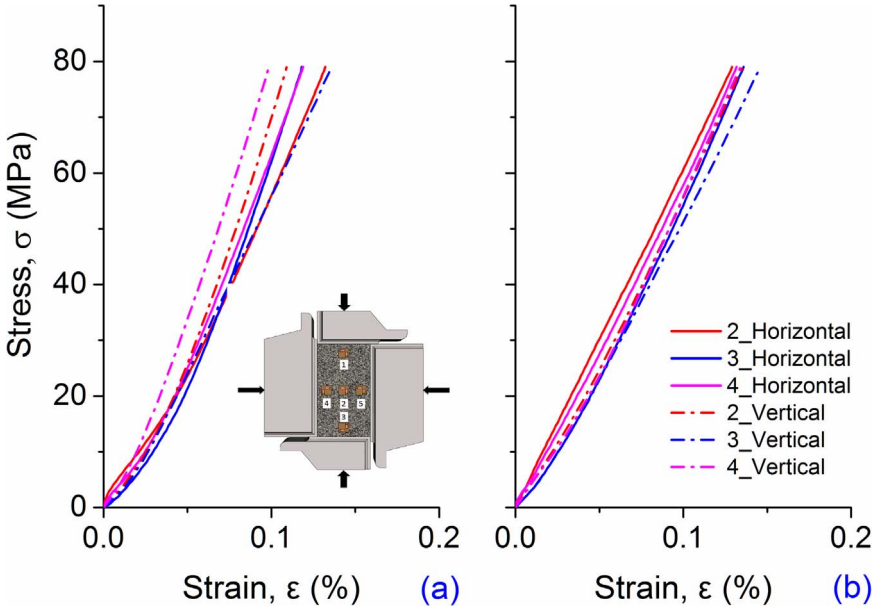

Fig. 3. Stress–strain curves under biaxial loading: (a) without any anti-friction agent; (b) with the MSV anti-friction agent.

mens without an anti-friction agent are plotted in Fig. 3(a). Pronounced scatter can be observed in these curves due to end friction effect. The compression strain varied from 0.098% to 0.136%; the deformation of points 4 in the vertical direction is smaller than the mean value. In contrast, the deformation of points 3 in the horizontal direction is larger than the mean value; this result is attributed to the end friction from the relative motion during biaxial loading. The MSV was used in this biaxial loading testing to reduce the influence of the end friction, and the results are presented in Fig. 3(b). The compression strain varied from 0.128% to 0.145%, which shows that the scatter feature is diminished.

5. Verification tests

5.1. End friction effect in the uniaxial compression tests

To assess the influence of the end friction effect and the different anti-friction agents on the strength and deformation, uniaxial compressive strength tests were performed on granite and marble specimens, six samples of each rock were tested, all of which were taken from the same block sample. The cylinder specimens were machined to 49 mm in diameter and 100 mm in height. The mean uniaxial compression strengths of the granite specimens without an anti-friction agent, with one-layer Teflon sheet, and with the MSV are 171.05, 153.02 and 161.42 MPa, respectively.

The end friction effect produces an increase in strength. However, the lowest strength corresponds to the specimens tested using the Teflon sheet rather than to those tested using the MSV. The corresponding strength change was observed in the tests on the marble; the results are presented in Table 1. For two types of rock, an increase of approximately 5.9–8.8% in the strength when using the MSV (the target standard), and a decrease of approximately 5.2–5.9% in the strength when Teflon was used. Representative stress–strain curves for the granite specimen are shown in Fig. 4. The end friction clearly affects the deformation behaviour both axially and radially. The Young's modulus is higher than that of the tests using the anti-friction agents, and the influence of the Poisson's ratio is not significant. The use of MSV is suggested in true triaxial tests based on these observed deformation and strength influences.

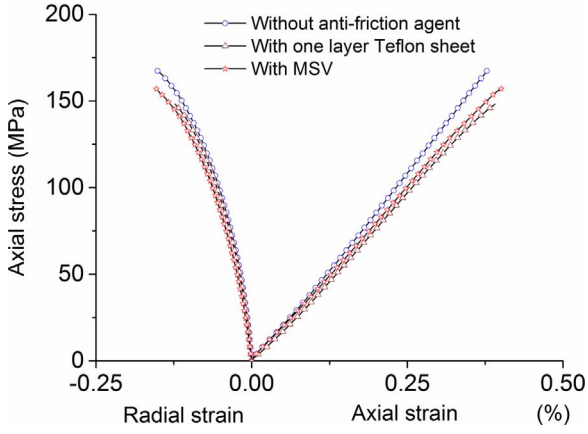

Fig. 4. Stress–strain curves of granite specimen from uniaxial compression tests.

5.2. End friction effect in the true triaxial tests

Comparative tests were performed on granite and sandstone specimens with MSV and without anti-friction agents under true triaxial conditions. The strain measurement method refers to that used in [20]. One set of typical data for two granite specimens and

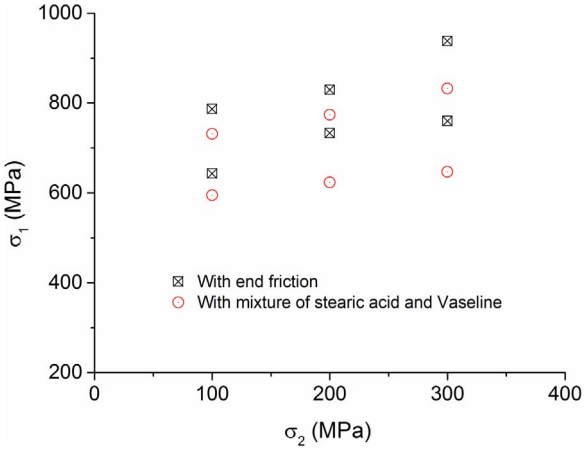

Fig. 6. Effect of end friction on rock strength of granite specimens under different intermediate principal stresses.

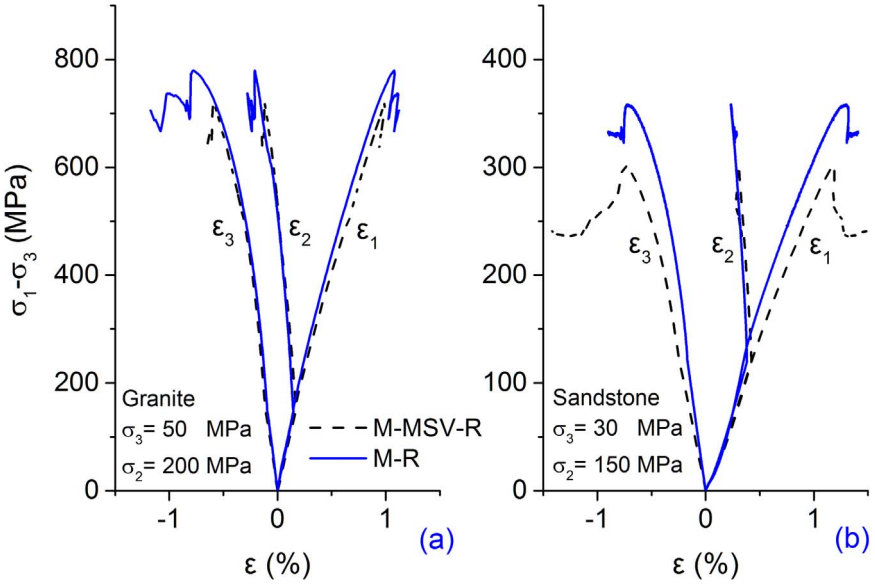

Fig. 5. Effect of end friction on the stress–strain relationship in true triaxial tests with and without anti-friction agents: (a) granite specimens; (b) sandstone specimens.

two marble specimens is selected to demonstrate the effect of end friction in true triaxial tests. The deviator stress (σ_1-σ_3) vs. strain (ε_1, ε_2 and ε_3) relationship is shown in Fig. 5(a) and (b). The solid blue M-R line denotes direct contact between the alloy steel platens and rock, and the dashed black M-MSV-R line denotes the use of an anti-friction agent.

An apparent increase in strength can be observed in both the granite and sandstone results when no anti-friction agent is used, which shows that the end friction promotes an artefactual increase in strength and that its function is equivalent to a slight improvement in the minor principal stress. The end friction affects the deformation. In the biaxial loading stage, the end friction suppresses ε_1 and ε_2, which leads to a steeper slope in the stress–strain curve. ε_3 is not affected, which could be because the measuring point is outside of the metal and rock interface. In the following shear stage, the Young's modulus is increased slightly due to friction; meanwhile, the minor principal strain is significantly released via the anti-friction agent because ε_3 is governed by four metal-rock interfaces under high compression stress. The Poisson's ratio is not markedly affected, as the major and minor deformations were restrained simultaneously.

The effect of end friction on the strength of the granite specimen under different intermediate principal stresses is shown in Fig. 6. The intermediate principal stresses were 100, 200 and 300 MPa under σ_3 for the cases of 30 and 50 MPa. Higher peak strengths were observed when the interfaces of the alloy steel platens and rock caused friction in all cases. The peak strength is generally 12–15% higher than that of the decreasing end friction. Higher σ_3 values tend to reduce the influence of the friction; however, higher σ_2 values increase the influence of the friction, which produces a higher strength.

6. Conclusions

This paper describes an experimental study on the effect of end friction in true triaxial tests on various types of rock. The primary aim was to verify the existing overestimated strengths obtained in many rock compressive tests due to the mismatch in the elasticity parameters (Young's modulus and Poisson's ratio) between alloy steel platens and rocks and to identify a proper anti-friction agent for use in true triaxial tests.

A multi-point strain measurement method is proposed to evaluate the change in the elastic strain distribution induced by the end friction effect. The experimental observations suggest that the MSV anti-friction agent is suitable for use in true triaxial and conventional triaxial tests. Further investigation is needed to optimize the proportion of MSV to reduce the friction coefficient.

Acknowledgements

The authors acknowledge the financial support provided by the National Natural Science Foundation of China under grant no. 11572083. The work in this paper was partially supported by the National Higher Education Institution for General Research and Development Funding (N120401007). The second author wishes to thank the China Scholarship Council (CSC) for supporting this research on rock mechanics at McGill University as a visiting scholar.

References

[1] Von Kármán T. Festigkeitsversuche unter allseitigem Druck. *Z Ver Dt Ing*. 1911;55:1749–1757.
[2] Föppl A. Abhangigkeit der Bruchgefahr von der Art des Spannungszustandes. *Mitth Mech Tech Lab K Tech Hochsch München*. 1900;27:1–35.
[3] Wawersik WR. Detailed Analysis of Rock Failure in Laboratory Compression Tests [Doctoral Thesis], Minneapolis, MN: University of Minnesota; 1968.
[4] Mogi K. Effect of the Triaxial Stress System on the Failure of Dolomite and Limestone. *Tectonophysics*. 1971;11:111–127.
[5] Mogi K. Fracture and flow of rocks under high triaxial compression. *J Geophys Res*. 1971;76:1255–1269.
[6] Brady BT. Initiation of failure in a radially end-constrained circular cylinder of brittle rock. *Int J Rock Mech Min Sci Geomech Abstr*. 1971;8:371–387.
[7] Filon LNG. On the elastic equilibrium of circular cylinders under certain practical systems of load. *Philos Trans R Soc Lond Ser A*. 1902;198:147–233.
[8] Peng SD. Stresses within elastic circular cylinders loaded uniaxially and triaxially. *Int J Rock Mech Min Sci Geomech Abstr*. 1971;8:399–432.
[9] Al-Chalabi M, Huang CL. Stress distribution within circular cylinders in compression. *Int J Rock Mech Min Sci Geomech Abstr*. 1974;11:45–56.
[10] Labuz J, Bridell JM. Reducing frictional constraint in compression testing through lubrication. *Int J Min Geol Eng Abstr*. 1993;30:451–455.
[11] Fairhurst C, Hudson J. Draft ISRM suggested method for the complete stress-strain curve for intact rock in uniaxial compression. *Int J Rock Mech Min Sci*. 1999;36:279–289.
[12] ASTM International. ASTM D7012-14 - standard test methods for compressive strength and elastic moduli of intact rock core specimens under varying states of stress and temperatures. West Conshohocken, PA: ASTM International; 2014.
[13] Galic D, Glaser SD, Goodman RE. A Lagrangian dynamic analysis of end effects in a generalized shear experiment. *Int J Rock Mech Min Sci*. 2008;45:495–512.
[14] Iwamoto T, Yokoyama T. Effects of radial inertia and end friction in specimen geometry in split Hopkinson pressure bar tests: a computational study. *Mech Mater*. 2012;51:97–109.
[15] Haimson B, Rudnicki JW. The effect of the intermediate principal stress on fault formation and fault angle in siltstone. *J Struct Geol*. 2010;32:1701–1711.
[16] Mogi K. Effect of the intermediate principal stress on rock failure. *J Geophys Res*. 1967;72:5117–5131.
[17] Haimson B, Chang C. A new true triaxial cell for testing mechanical properties of rock, and its use to determine rock strength and deformability of Westerly granite. *Int J Rock Mech Min Sci*. 2000;37:285–296.
[18] Ingraham MD, Issen KA, Holcomb DJ. Response of Castlegate sandstone to true triaxial states of stress. *J Geophys Res Solid Earth*. 2013;118:536–552.
[19] Nasseri MHB, Goodfellow SD, Young RP. 3-D transport and acoustic properties of Fontainebleau sandstone during true-triaxial deformation experiments. *Int J Rock Mech Min Sci*. 2014;69:1–18.
[20] Feng X-T, Zhang X, Kong R, Wang G. A novel Mogi type true triaxial testing apparatus and its use to obtain complete stress–strain curves of hard rocks. *Rock Mech Rock Eng*. 2016;49:1649–1662.
[21] Mogi K. Experimental Rock Mechanics, London: Taylor & Francis; 2007.
[22] Cai M. Influence of intermediate principal stress on rock fracturing and strength near excavation boundaries - Insight from numerical modeling. *Int J Rock Mech Min Sci*. 2008;45:763–772.
[23] Li X, Shi L, Bai B, Li Q, Xu D, Feng X. True-triaxial testing techniques for rocks—state of the art and future perspectivesKwasniewski M, Li X, Takahashi M, eds. True Triaxial Testing of Rocks, Boca Raton, FL: CRC Press; 2012, pp.3–18.
[24] Pan PZ, Feng XT, Hudson JA. The influence of the intermediate principal stress on rock failure behaviour: a numerical study. *Eng Geol*. 2012;124:109–118.
[25] Bowden FP. Friction. *Nature*. 1950;166:330–334.
[26] Li J, Zhang C, Deng M, Luo J. Reduction of friction stress of ethylene glycol by attached hydrogen ions. *Sci Rep*. 2014;4:7226.
[27] Ferrero AM, Migliazza MR. Theoretical and numerical study on uniaxial compressive behaviour of marl. *Mech Mater*. 2009;41:561–572.
[28] Linker MF, Dieterich JH. Effects of variable normal stress on rock friction: observations and constitutive equations. *J Geophys Res*. 1992;97:4923–4940.
[29] Peng S, Johnson AM. Crack growth and faulting in cylindrical specimens of Chelmsford granite. *Int J Rock Mech Min Sci Geomech Abstr*. 1972;9:37–86.
[30] Das MN. Influence of width/height ratio on post-failure behaviour of coal. *Int J Min Geol Eng*. 1986;4:79–87.
[31] Özkan I, Özarslan A, Geniş M, Özşen H. Assessment of scale effects on uniaxial compressive strength in rock salt. *Environ Eng Geosci*. 2009;15:91–100.
[32] Thuro K, Plinninger RJ, Zäh S, Schütz S. Scale effects in rock strength properties. part 1: unconfined compressive test and Brazilian testSärkkä P, Eloranta P, eds. Rock Mechanics–A Challenge for Society, London: CRC Press; 2001, pp.169–174.
[33] Tang CA, Tham LG, Lee PKK, Tsui Y, Liu H. Numerical studies of the influence of microstructure on rock failure in uniaxial compression—part II: constraint, slenderness and size effect. *Int J Rock Mech Min Sci*. 2000;37:571–583.